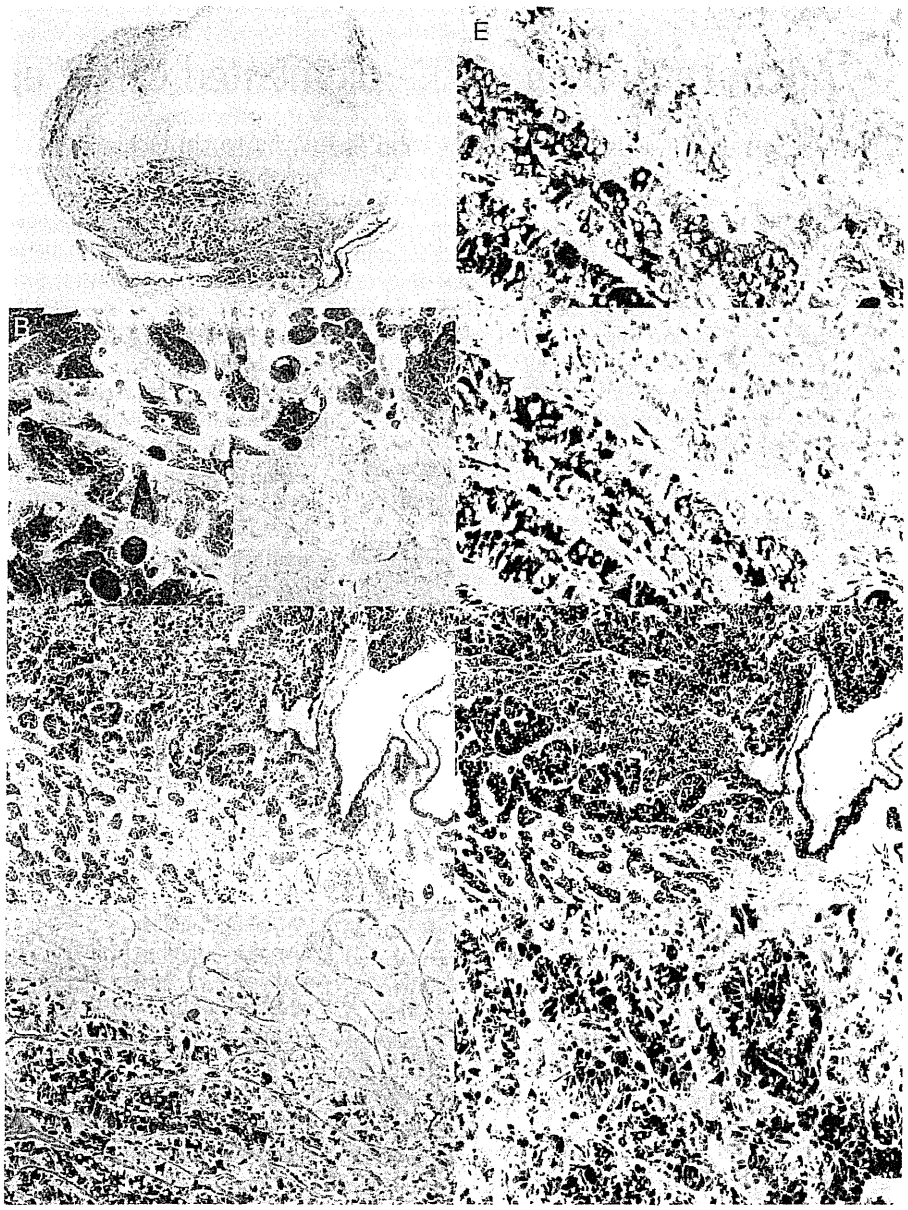

Figure 2 Microscopic features and immunohistochemical features. The tumour had pigmented and non-pigmented areas (A; low magnification). Both the pigmented area (B; high magnification) and the non-pigmented area (inset) showed the presence of epithelioid cells surrounding thin marked vessels. The invasive site of tumour cells and background ciliary epithelium stained with H&E (C). The tumour basement membrane surrounding the glands was positive for periodic acid-Schiff staining (D). the micrograph after counterstaining with Giemsa stain Melan A (E) and microphthalmia-associated transcription factor (F). The tumour had positive reactivity to the pancytokeratin OSCAR (G) and cytokeratin 7 (H) detected by performing alkaline phosphatase staining.

The tumour had grown endophytically, with invasion into the subepithelial stroma of the ciliary body (figure 2C). The tumour consisted of epithelial cells with moderate pleomorphic nuclei and prominent nucleoli. The tumour showed a nested, cord and glandular pattern. Periodic acid-Schiff (PAS) staining revealed that the tumour had a clearly glandular pattern with a prominent basement membrane surrounding the glands (figure 2D).

Immunohistochemical findings

Immunohistochemical studies showed that the tumour cells were diffusely and strongly positive for S100, Melan A and microphthalmia-associated transcription factor (MITF) (figure 2E, F); were focally positive for EMA, showed no reactivity to cytokeratin CAM5.2; and were diffusely positive for OSCAR (figure 2G) and weakly positive for cytokeratin AE1/AE3 and cytokeratin 7 (figure 2H) HMB45 was positive in only the cells with brownish granules. The Ki-67 labelling index contributed to the diagnosis. A minimum of 1000 tumour nuclei were counted in this case. The Ki-67 index was 11%.

INVESTIGATIONS

Formalin-fixed paraffin-embedded specimens were cut into 4 μm thick sections. Deparaffinised sections were subjected to H&E and immunohistochemical staining. Immunohistochemical

staining was performed with the following primary antibodies: cytokeratin AE1/AE3, cytokeratin 7 (1:100; Dako, Glostrup, Denmark), cytokeratin OSCAR (1:100; Signet), cytokeratin CAM5.2 (1:20; Becton Dickinson Immunocytometry Systems, San Jose, California, USA), EMA (1:100; Dako); E29 (Dako), S100 (1:2000; rabbit polyclonal, Dako), HMB45 (1:10; Dako), Melan A (1:100; A103, Dako), MITF; 1:100; D5, Dako) and Ki-67 (1:100; MIB-1, Dako). Each section was exposed to 0.3% hydrogen peroxide for 15 min to block endogenous peroxidase activity. For staining, we used an automated stainer (Dako) according to the manufacturer's protocol. ChemMate EnVision HRP/DAB and G2 system AP kits (Dako) and counterstaining with giemsa were used for detection. Appropriate positive and negative controls were used for each antibody. Nuclear staining of the tumour cells was checked for positivity of S100, MITF, and Ki-67, and cytoplasmic staining was checked for positivity of cytokeratins, EMA, HMB45 and Melan A.

DIFFERENTIAL DIAGNOSIS

Epithelioid cell-type melanomas.

TREATMENT

Science the size of the lesion increased and MRI indicated 'adenoma' 3 months after presentation, the ciliary body was resected without eyeball enucleation.

OUTCOME AND FOLLOW-UP

No recurrence and metastasis was observed during a 9 -month follow-up period.

DISCUSSION

In the present case, the tumour cells showed a high degree of melanogenesis, with pancytokeratin (OSCAR), CK7, Melan A, HMB45 and MITF immunopositivity. The pigmented epithelial cells of the iris, ciliary body and retina as well as melanocytes show melanogenesis. It is difficult to distinguish benign and malignant tumours of pigmented and non-pigmented ciliary epithelia from malignant melanoma of the ciliary body through clinical examination. Malignant melanoma has to be excluded via histological examination. Cytokeratin or EMA expression in either pigmented or non-pigmented neoplasms of the ciliary epithelium was reported to be focal or mild.[3]

Some cases of adenocarcinoma of the pigmented or non-pigmented ciliary epithelium have been reported to express S100, a well-known marker of melanocytic tumours.[3] In our case, expression of Melan A, HMB45 and MITF, known markers of melanocytic tumours, were positive.[4] Microphthalmia transcription factor (MITF) is essential in normal melanocyte development, and it controls the expression of pigmented cell phenotypes. The application of MITF and HMB45 as markers in the diagnosis of melanoma has been extensively studied. This is the first report of a pigmented ciliary adenocarcinoma being positive for MITF and HMB45. Therefore, comprehensive evaluation of parameters including morphology, imaging results and clinical information is required for proper diagnosis. The criterion used for the diagnosis and differentiation of adenoma arising from the ciliary pigmented epithelium is local invasion to the iris, ciliary body stroma, anterior chamber angle and sclera.[1] In the present case, the tumour clearly invaded the ciliary body stroma around the vessels and showed moderate pleomorphism. In addition, the Ki-67 and mitotic indices might indicate malignant behaviour.

The prognosis of adenocarcinoma of the pigmented ciliary epithelium has not been elucidated. Although the tumours have been described as showing extraocular extension and metastasis to other organs in a few case reports, tumour relapse or metastasis after tumour resection or enucleation of the eye has not been reported.[5] Adenocarcinoma of the pigmented ciliary epithelium seems to have a relatively good prognosis compared with malignant melanoma.

A pathologist who encounters a tumour arising from the ciliary body with evidence of melanogenesis should be attentive to the existence of epithelial features in order to differentiate adenocarcinoma of the pigmented epithelium from malignant melanoma.

Learning points

- Adenocarcinoma of the pigmented ciliary epithelium is an exceptionally rare malignant eye tumour.
- This tumour was positively immunostained for pancytokeratin (OSCAR), Melan-A, S-100, HMB45 and microphthalmia-associated transcription factor.
- Diagnosis of pigmented eye neoplasms requires comprehensive evaluation of many parameters including the morphology, MRI findings and immunohistochemical results.

Acknowledgements The authors are grateful to Dr Yukiko Aihara, Dr Miyuki Fujiwara, Dr Ryoji Kushima and Dr Akiko Maeshima for supporting this work and Ms Sachiko Miura and Ms Chizu Kina for their skilled technical assistance.

Contributors AS and TM designed the manuscript and made the diagnosis. AO made the pathological diagnosis and SS provided the clinical data.

Competing interests None.

Patient consent Obtained.

Provenance and peer review Not commissioned; externally peer reviewed.

REFERENCES

1 Font RL, Croxatto JO, Rao NA. AFIP atlas of tumor pathology, 4th series fascicle 5: tumors of the eye and ocular adnexa Washington, DC: AFIP, 2006.
2 Zimmerman LE. Verhoeff's terato-neuroma a critical reappraisal in light of new observations and current concepts of embryonic tumors. *Trans Am Ophthalmol Soc* 1971:69:210–36.
3 Laver NM, Hidayat AA, Croxatto JO. Pleomorphic adenocarcinomas of the ciliary epithelium. Immunohistochemical and ultrastructural features of 12 cases. *Ophthalmology* 1999:106:103–10.
4 King R, Weilbaecher KN, McGill G, *et al*. Microphthalmia transcription factor. A sensitive and specific melanocyte marker for MelanomaDiagnosis. *Am J Pathol* 1999:155:731–8.
5 Rodrigues M, Hidayat A, Karesh J. Pleomorphic adenocarcinoma of ciliary epithelium simulating an epibulbar tumor. *Am J Ophthalmol* 1988:106:595–600.

Society For Biomaterials

Basic study of soft tissue augmentation by adipose-inductive biomaterial

Masaki Yazawa,[1] Taisuke Mori,[2] Yasuhide Nakayama,[3] Kazuo Kishi[1]

[1]Department of Plastic and Reconstructive Surgery, School of Medicine, Keio University, Tokyo, Japan
[2]Department of Pathology, National Cancer Center Laboratory, Tokyo, Japan
[3]Division of Medical Engineering and Materials, National Cerebral and Cardiovascular Center Research Institute, Osaka, Japan

Received 19 December 2013; revised 25 February 2014; accepted 12 April 2014
Published online 00 Month 2014 in Wiley Online Library (wileyonlinelibrary.com). DOI: 10.1002/jbm.b.33180

Abstract: Reconstructive surgery for tumor resection, trauma, and congenital anomaly involves volume augmentation with autologous tissue transfer. However, a healthy region is damaged as a donor site, and the autologous tissue is transferred like a patchwork to the recipient site. We have attempted to induce adipogenesis activity in artificial biomaterial that is injectable with an injection needle for soft tissue augmentation. First of all, the optimal dose of pioglitazone hydrochloride was examined with adipo-precursor cells in terms of the proliferator-activated receptor-γ mRNA expression levels affected by reagent *in vitro*. Then, salmon collagen with pioglitazone was adjusted in terms of the dose and the salmon collagen was injected into mouse back using an injection needle *in vivo*. At 4 weeks after implantation, the pioglitazone collagen gel was substituted by mature adipocytes in comparison with the case for control collagen gel without pioglitazone. These results are indicative of the possibility of promoting adipogenesis using collagen with pioglitazone as an adipose-inductive substance. © 2014 Wiley Periodicals, Inc. J Biomed Mater Res Part B: Appl Biomater 00B: 000–000, 2014.

Key Words: adipose, biomaterial, augmentation, soft tissue

How to cite this article: Yazawa M, Mori T, Nakayama Y, Kishi K. 2014. Basic study of soft tissue augmentation by adipose-inductive biomaterial. J Biomed Mater Res Part B 2014:00B:000–000.

INTRODUCTION

In recent years, advances in medicine have spectacularly improved the survival rate in tumor resection, trauma, and congenital anomaly. However, some patients cannot obtain a sufficient quality of life because of poor appearance after treatments. At present, reconstructive surgery for tumor resection, trauma, and congenital anomaly involves volume augmentation with autologous tissue transfer. However, a healthy region is damaged as a donor site, and the autologous tissue is transferred like a patchwork to the recipient site. Therefore, the quality of life of patients is not improved sufficiently.

Now, a new tissue transfer method without the problems at donor and recipient sites is required. We have attempted to induce adipogenesis activity in artificial biomaterial that is injectable using an injection needle, with the goal of its clinical application. To achieve this, pioglitazone hydrochloride was selected because it has been applied in clinical treatment as a diabetic medicine and has been reported to induce adipogenesis via peroxisome proliferator-activated receptor-γ (PPAR-γ).[1,2]

As an injectable artificial biomaterial, salmon collagen was selected because it is clinically available and should work as a scaffold for adipose tissue by ligand protein interaction.[3–7]

First of all, the optimal dose of pioglitazone was examined. Then, salmon collagen with pioglitazone was adjusted in terms of the dose and the salmon collagen was injected using an injection needle *in vivo*. Finally, adipogenesis at the recipient site was estimated in terms of the function of the artificial material as a transplant bed for adipogenesis.

MATERIALS AND METHODS

Animal care

The experimental procedure was authorized and reviewed by the Keio University Experimental Animal Center Committee (Approval no. 10256(0)).

Forty C3H/He/N mice (8 weeks, male, body weight 25–30 g; purchased from Charles River Laboratories Japan Inc., Tokyo, Japan) were used in the current study. All surgeries were performed in an animal-operating suite at the university.

Histological analysis

All tissue samples were obtained by mouse experiment and were fixed in 10% formalin and embedded in paraffin.

Correspondence to: M. Yazawa (e-mail: prsyazawa@gmail.com)
Contract grant sponsor: Japan Society for the Promotion of Science; contract grant number: KAKENHI 23792059

Subcutaneous transplanted materials were histologically evaluated.

Adipose precursor isolation and cell culture

To study adipo-precursor cells in terms of their PPAR-γ mRNA expression levels induced by the reagent *in vitro*, we isolated cells from the subcutaneous fat pad tissue of mice at a lower-back site. Briefly, tissue was minced and incubated for 1 h at 37°C in a rotary shaking bath at 100 rpm in digestion buffer containing collagenase (5 mg/mL) before being filtered through a 400-μm nylon mesh. The adipo-precursor cells were washed twice with serum-free Dulbecco's modified Eagle's medium (DMEM) (pH 7.4, 10 n*M* 4-(2-hydroxyethyl)-1-piperazineethanesulfonic acid (HEPES), containing penicillin/streptomycin) and incubated at 37°C under sterile tissue culture conditions. The adipo-precursor cells were expanded in bulk culture to avoid any biases resulting from cloning, and subjected to further analysis.

For cell proliferation assay, we used "passage two" adipose precursor cells as this would eliminate the hematocytes. About 1×10^5 cells were seeded into six cell culture plates in triplicate and counted at 14 days. For the induction of PPAR-γ mRNA expression, 100, 10, and 1 μ*M* pioglitazone (pioglitazone hydrochloride, Tokyo Chemical Industry, Tokyo, Japan), 200, 20, and 2 ng/mL insulin-like growth factor (IGF) 1 (PeproTech, NJ), and 200, 20, and 2 ng/mL IGF2 (PeproTech, NJ) were each added to the culture medium.

Quantitative reverse transcription PCR

Total RNAs were extracted with the RNeasy Mini kit (Qiagen, Valencia, CA) and reverse-transcribed using the SuperScript III RT-PCR system (Invitrogen, Carlsbad, CA) according to the manufacturer's protocol. We did not change the media for 2 weeks for the induction of adipocytes. One microliter of cDNA sample was amplified by PCR gene-specific primers. For quantitative RT-PCR (qRT-PCR), reactions were performed in triplicate using Fast Start Universal Probe Master (Roche Applied Science, Penzberg, Germany). The primer sets were as follows: for mouse PPAR-γ: 5′-ATCATCTACACGATGCTGGCC-3′ (forward), 5′-CTCCCTGGTCATGAATCCTTG-3′ (reverse); and for GAPDH: 5′-CACCATGGAGAAGGCCGGGG-3′ (forward), 5′-GACG GACACATTGGGGGTAG-3′ (reverse).

Statistical analysis

Data are expressed as mean ± SE (standard error). The relative mRNA expression levels were compared using unpaired *t*-test and all statistical analyses were performed using Statcel software (OSM, Japan). The results were judged significant at $p < 0.05$.

Adipogenesis by artificial biomaterial with pioglitazone *in vivo*

Nine C3H/He/N mice were used and maintained under specific pathogen-free conditions throughout this experiment. The optimal dose of pioglitazone was determined to be 10 μ*M* by previous cell proliferation assays. About 0.5% salmon collagen particles with and without pioglitazone (10 μ*M*) (0.9 g each, both from IHARA & Co., Ltd., Japan) were produced as follows. The salmon atelocollagen W/O (water in oil) emulsion was made by span20 (sorbitan monolaurate). The salmon collagen crosslinked by EDC (1-ethyl-3-(dimethylaminopropyl) carbodiimide hydrochloride) was settled down as particles to the water phase of 50% (vol/vol) EtOH. Dried particles were mixed with pioglitazone (10 μ*M*) solution and aspirated. The collagen particles with and without pioglitazone were dispersed in 0.9 mL of saline. About 0.1 mL of collagen gel with and without pioglitazone was injected under bilateral dorsal skin layer using an 18-G injection needle. The mice were then sacrificed and evaluated pathologically at 1, 2, and 4 weeks after operation. Three replicate samples were performed for each test. In addition, the area of adipose tissue was calculated in the histologic sections using software (Photoshop 7.0, Adobe, USA).

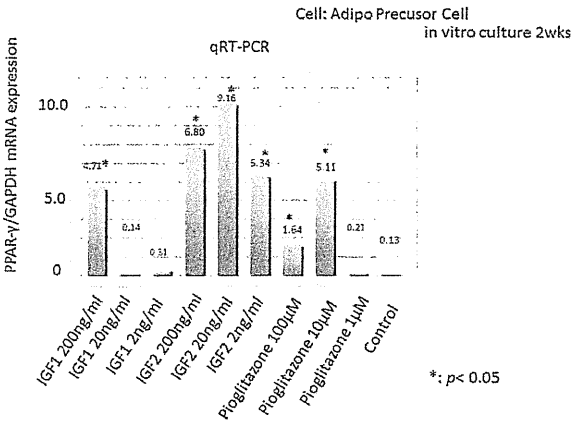

FIGURE 1. Pioglitazone and IGFs up-regulated PPAR-γ mRNA levels in mouse adipo-precursor cells. Mouse adipo-precursor cells were incubated for 2 weeks with pioglitazone, IGF1, or IGF2 at the indicated doses, and PPAR-γ mRNA levels were determined by qRT-PCR. *$p < 0.05$ versus control. [Color figure can be viewed in the online issue, which is available at wileyonlinelibrary.com.]

RESULT

Pioglitazone and IGFs up-regulated PPAR-γ mRNA levels

PPAR-γ is considered to be one of the master regulators of adipocyte differentiation (Figure 1).[8] To evaluate the potential effects of pioglitazone and IGFs on PPAR-γ expression, we exposed mouse adipo-precursor cells to these substances for 2 weeks and performed qRT-PCR. As shown in Figure 1, the dose responses of the expression level of PPAR-γ mRNA with pioglitazone, IGF1, IGF2, and control (without any reagent) were quantitatively analyzed in cultured cells. The PPAR-γ expression levels were efficiently up-regulated dose-dependently by all reagents, whereas 100 μ*M* pioglitazone caused cell toxicity (mean relative levels: pioglitazone 1 μ*M* vs. 10 μ*M* vs. 100 μ*M* = 0.21 vs. 5.11 vs. 1.64; mean relative levels: IGF1 2 ng/mL vs. 20 ng/mL vs. 200 ng/mL = 0.31 vs. 0.14 vs. 4.71; mean relative levels: IGF2 2 ng/mL vs. 20 ng/mL vs. 200 ng/mL = 5.34 vs. 9.16 vs. 6.80). The effective induction abilities of PPAR-γ by pioglitazone

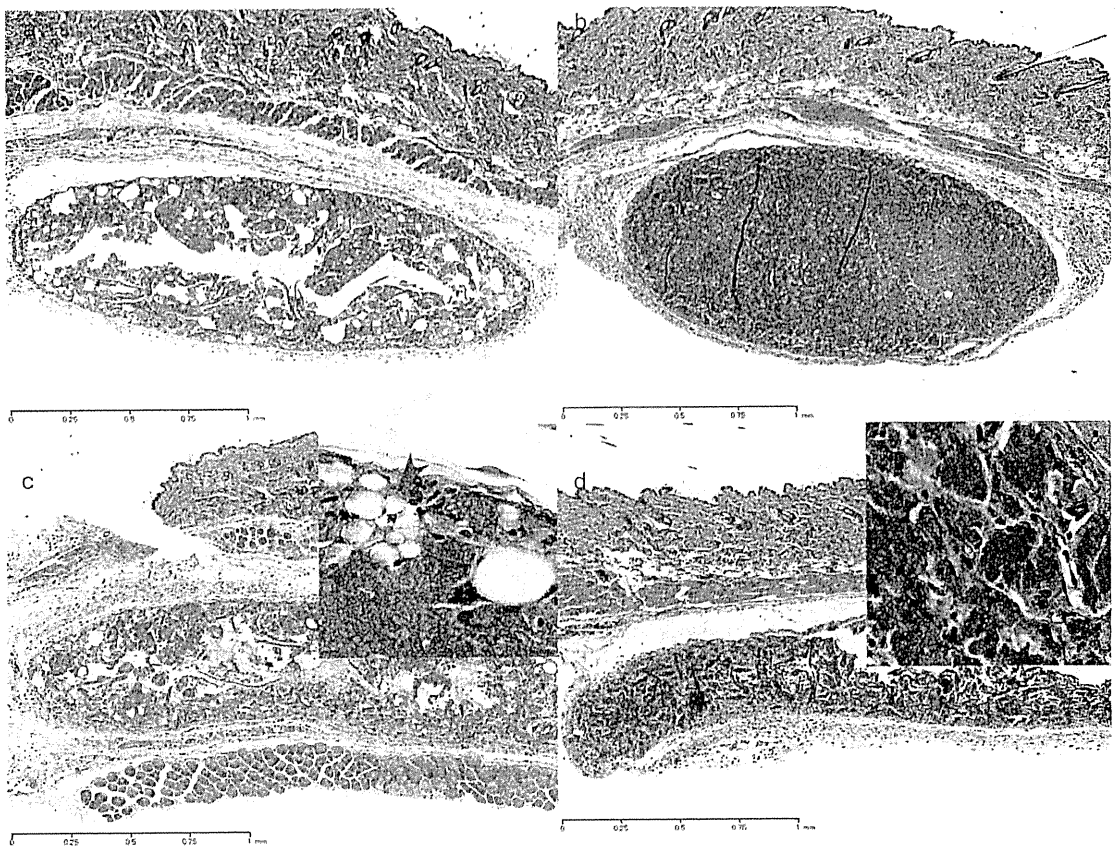

FIGURE 2. Photomicrographs of sections from implanted collagen gel after 1 week and 4 weeks. At 1 week after implantation, both the collagen gels were observed without any immune elimination (a, b). At 4 weeks after implantation, the pioglitazone collagen gel (c) was substituted by mature adipocytes (arrow heads) in comparison with the case for control gel (d). (a, c) Collagen gel with pioglitazone at 10 μM; (b, d) collagen gel only (H&E staining, original magnification 100× and insets 400×). [Color figure can be viewed in the online issue, which is available at wileyonlinelibrary.com.]

and IGFs were not significantly different from the control ($n = 3$; $p > 0.05$).

Quantification of induced adipose tissue *in vivo*

We evaluated the time course of the areas of adipose tissue induced by pioglitazone/collagen gel (induced group) that was comprised of mature adipose cells relative to the total implanted gel area (Figures 2 and 3). For mature adipose cells observed at the edge of the pioglitazone/collagen gel after one week of implantation, the average area percentage was 4.29%. In contrast, few adipose cells were observed in the collagen gels without pioglitazone (control group); the average area percentage was 0.343%. The collagen gels without pioglitazone as a control began to degrade without the induction of adipose cells from 2 weeks. In contrast, in the collagen gels with pioglitazone as an induced group, the replacement of adipose cells was observed. The induced group had higher proportions of adipose cells in the gels in a time-dependent manner after 2 weeks and 4 weeks. The average area percentages were 5.36% in the induced group and 0.394% in the control group after 2 weeks. They were 17.7% in the induced group and 1.20% in the control group after 4 weeks, as shown in Figure 3. There were statistically significant differences between the induced group and the control group ($p < 0.05$).

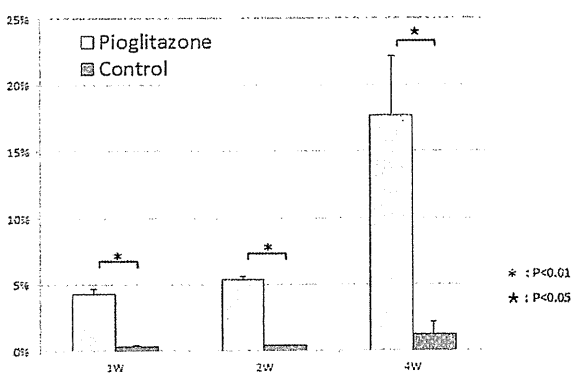

FIGURE 3. Area percentages of induced adipose tissue *in vivo*. [Color figure can be viewed in the online issue, which is available at wileyonlinelibrary.com.]

DISCUSSION

In the field of reconstructive surgery, operative techniques for autologous tissue transfer and medical technology in artificial materials have improved. To obtain autologous tissue, however, there is still a need for a donor site in a healthy body area, which is sutured to the recipient site like a patchwork for volume augmentation. This is not ideal in terms of patient satisfaction. In the case of hard tissue, artificial bone has already been developed into block and liquid types with processability for clinical applications, while liquid artificial bone is injectable with an injection syringe. On the other hand, in the case of soft tissue, various methods have been reported for fat augmentation.[9,10] However, these reports require a healthy donor site and the obtained results have not always been stable in the long-term. For example, fat tissue is taken from a small incision at a healthy area of a patient by suction and the fat tissue is injected into the recipient area of the patient using a syringe.[11] Besides, Kimura et al. reported a combination method involving autologous fat cells and artificial material.[12] The volume rate of grafted fat tissues is, nevertheless, unstable and unpredictable, with most of the volume being absorbed as time passes. These lines of evidence indicate the possibility of repetitive operations and overdose of fat grafting. These conventional methods for autologous fat grafting always need a healthy donor site and the patient is subjected to an invasive burden by repetitive operations. As such, the development of a new approach for soft tissue augmentation has long been anticipated internationally.

In this study, our ideas were based on our previous report that mesenchymal stromal cells induced adipocytes.[13] For an adjunct to artificial biomaterial, pioglitazone hydrochloride was focused on as a substance for adipose induction and maintenance.[14–16] Youm et al. reported that pioglitazone induces ectopic adipogenesis via PPAR-γ.[1] Pioglitazone hydrochloride is already used for diabetic patients in clinical applications.

Therefore, the optimal concentration of pioglitazone for the efficient induction and promotion of adipose tissue was examined. The mRNA levels of PPAR-γ, which is considered to be one of the master regulators of adipocyte differentiation,[17] were examined by qRT-PCR *in vitro*. IGF1 and IGF2 were used for comparison. The concentrations of each substance, pioglitazone, IGF1, and IGF2, were set at three levels using examples from previous reports.[18,19] It was found that 10 μM pioglitazone was associated with a significantly high PPAR-γ mRNA level for adipo-precursor cells (Av. 5.11, $p < 0.05$). In addition, 100 μM pioglitazone was associated with a significant difference from the control, but was lower than that for 10 μM (Av. 1.64, $p < 0.05$). The effect of 1 μM pioglitazone was almost the same as the control (Av. 0.21). About 10 μM was thus set as the optimal concentration of pioglitazone for adipogenesis of adipo-precursor cells. Next, pioglitazone was compared with IGF1 and IGF2. It is interesting to note that all levels of IGF2 were associated with very high levels of PPAR-γ mRNA (2 μM: Av. 5.34; 20 μM: Av. 9.16; 200 μM: Av. 6.80). In the examination of the effect of IGF1 on the PPAR-γ mRNA level, 200 μM was the only level to show a significant difference from the control (Av. 4.71, $p < 0.05$). About 10 μM pioglitazone was associated with similar PPAR-γ mRNA expression to IGF1 and IGF2, which are known to be PPAR-γ inducers. These results indicated that 10 μM pioglitazone is reasonable as the optimal level for inducing PPAR-γ mRNA expression.

This study was intended to aid the development of clinical applications, so 10 μM pioglitazone was examined *in vivo*. Salmon collagen, as an injectable artificial biomaterial, was chosen here as it is clinically available and should work as a scaffold for adipose tissue by ligand protein interaction.[3–7] We think that the preferable size of collagen particles for scaffold of cell proliferation is between 70 μm and 130 μm in diameter, as the cells are between 10 μm and 20 μm in diameter. Our salmon collagen particles are, from our previous results, 223 μm or less in diameter on average. In terms of adjusting the salmon collagen, we chose 0.3–0.5% solution for the injectable component and included 10 μM pioglitazone. This conditioned collagen with or without pioglitazone was implanted into mouse back under the skin layer and observed over time. At 1 week after implantation, both the collagen gels were observed without any immune elimination. A small number of fat droplets were observed at the edge of the collagen gel with pioglitazone. At 4 weeks after implantation, the collagen gel with pioglitazone was substituted by mature adipocytes in comparison with the case for the collagen gel without pioglitazone. We think that the source of mature adipocytes in collagen gels is migrated mesenchymal stem cells or migrated adipo-precursor cells and that the nourishment for adipocytes in collagen gels is from both peripheral vessels and indirect diffusion. These results are indicative of the possibility of promoting adipogenesis by collagen supplemented with pioglitazone as an adipose-inductive substance.

In future, if larger volumetric adipogenesis becomes a reality, this result should be highly promising for the following factors:

1. Soft tissue augmentation after tumor resection;
2. Prevention of wound contracture and promotion of wound healing;
3. Prevention of perforation, scar formation, and stenosis of intestinal mucosa damaged by digestive endoscopy; and
4. Esthetic improvement of poor form caused by body surface asperity.

ACKNOWLEDGMENT

Authors thank Hatsumi Kobayashi and Masanobu Munekata (IHARA & Co., Ltd., Japan) for preparation of the salmon collagen with and without pioglitazone. The authors declare no conflicts of interest.

REFERENCES

1. Youm YH, Yang H, Amin R, Smith SR, Leff T, Dixit VD. Thiazolidinedione treatment and constitutive-PPARγ activation induces ectopic adipogenesis and promotes age-related thymic involution. Aging Cell 2010;9:478–489.
2. Schadinger SE, Bucher NLR, Schreiber BM, Farmer SR. PPARγ2 regulates lipogenesis and lipid accumulation in steatotic hepatocytes. Am J Physiol Endocrinol Metab 2005;288: 1195–1205.

3. Yunoki S, Nagai N, Suzuki T, Munekata M. Novel biomaterial from reinforced salmon collagen gel prepared by fibril formation and cross-linking. J Biosci Bioeng 2004;98:40–47.
4. Nagai N, Kubota R, Okahashi R, Munekata M. Blood compatibility evaluation of elastic gelatin gel from salmon collagen. J Biosci Bioeng 2008;106:412–415.
5. Nagai N, Nakayama Y, Zhou YM, Takamizawa K, Mori K, Munekata M. Development of salmon collagen vascular graft: Mechanical and biological properties and preliminary implantation study. J Biomed Mater Res B Appl Biomater 2008;87:432–439.
6. Nagai N, Nakayama Y, Nishi S, Munekata M. Development of novel covered stents using salmon collagen. J Artif Organs 2009; 12:61–66.
7. Kawaguchi Y, Kondo E, Kitamura N, Arakaki K, Tanaka Y, Munekata M, Nagai N, Yasuda K. In vivo effects of isolated implantation of salmon-derived crosslinked atelocollagen sponge into an osteochondral defect. J Mater Sci Mater Med 2011;22:397–404.
8. Rosen ED, Walkey CJ, Puigserver P, Spiegelman BM. Transcriptional regulation of adipogenesis. Genes Dev 2000;14:1293–1307.
9. Kelly JL, Findlay MW, Knight K, Penington A, Thompson EW, Messina A, Morrison WA. Contact with existing adipose tissue is inductive for adipogenesis in matrigel. Tissue Eng 2006;12:2041–2047.
10. Findley MW, Messina A, Thompson EW, Morrison WA. Long-term persistence of tissue-engineered adipose flaps on a murine model to 1 year: An update. Plast Reconstr Surg 2009;124:1077–1084.
11. Phulpin B, Gangloff P, Tran N, Bravetti P, Merlin JL, Dolivet G. Rehabilitation of irradiated head and neck tissue by autologous fat transplantation. Plast Reconstr Surg 2009;123:1187–1197.
12. Kimura Y, Ozeki M, Inamoto T, Tabata Y. Adipose tissue engineering based on human preadipocytes combined with gelatin microspheres containing basic fibroblast growth factor. Biomaterials 2003;24:2513–2521.
13. Allan EH, Ho PW, Umezawa A, Hata J, Makishima F, Gillespie MT, Martin TJ. Differentiation potential of a mouse bone marrow stromal cell line. J Cell Biochem 2003;90:158–169.
14. Kern PA, Marshall S, Eckel RH. Regulation of lipoprotein lipase in primary cultures of isolated human adipocytes. J Clin Invest 1985; 75:199–208.
15. Bodles AM, Banga A, Rasouli N, Ono F, Kern PA, Owens RJ. Pioglitazone increases secretion of high-molecular-weight adiponectin from adipocytes. Am J Physiol Endocrinol Metab 2006;291:E1100–E1105.
16. Yamanouchi K, Ban A, Shibata S, Hosoyama T, Murakami Y, Nishihara M. Both PPARγ and C/EBPα are sufficient to induce transdifferentiation of goat fetal myoblasts into adipocytes. J Reprod Dev 2007;53:563–572.
17. Gurnell M. Peroxisome proliferator-activated receptor gamma and the regulation of adipocyte function: Lessons from human genetic studies. Best Pract Res Clin Endocrinol Metab 2005;19:501–523.
18. Higashi Y, Holder K, Delafontaine P. Thiazolidinediones up-regulate insulin-like growth factor-1 receptor via a peroxisome proliferator-activated receptor gamma-independent pathway. J Biol Chem 2010;285:36361–36368.
19. Kleiman A, Keats EC, Chan NG, Khan ZA. Elevated IGF2 prevents leptin induction and terminal adipocyte differentiation in hemangioma stem cells. Exp Mol Pathol 2013;94:126–136.

Histopathology

Histopathology 2014, 65, 465–472. DOI: 10.1111/his.12405

Utility of PAX8 mouse monoclonal antibody in the diagnosis of thyroid, thymic, pleural and lung tumours: a comparison with polyclonal PAX8 antibody

Akane Toriyama,[1,2] Taisuke Mori,[1,3] Shigeki Sekine,[1,3] Akihiko Yoshida,[1] Okio Hino[4] & Koji Tsuta[1]

[1]*Division of Pathology and Clinical Laboratories, National Cancer Center Hospital, Tokyo, Japan,* [2]*Department of Pathology, Juntendo University Urayasu Hospital, Chiba, Japan,* [3]*Division of Pathology, National Cancer Center Research Institute, Tokyo, Japan, and* [4]*Department of Pathology and Oncology, Juntendo University School of Medicine, Tokyo, Japan*

Date of submission 26 November 2013
Accepted for publication 28 February 2014
Published online *Article Accepted* 4 March 2014

Toriyama A, Mori T, Sekine S, Yoshida A, Hino O & Tsuta K
(2014) *Histopathology* **65**, 465–472

Utility of PAX8 mouse monoclonal antibody in the diagnosis of thyroid, thymic, pleural and lung tumours: a comparison with polyclonal PAX8 antibody

Aims: The purpose of this study was to compare the immunohistochemical staining profiles of PAX8-polyclonal, PAX8-monoclonal, PAX5-monoclonal and PAX6-monoclonal antibodies in several histological types of primary thoracic and thyroid tumours. In addition, we analysed *PAX8* mRNA expression by using *in-situ* hybridization.

Methods and results: We compared polyclonal PAX8 and monoclonal PAX8, PAX5 and PAX6 antibodies in 962 samples (687 lung carcinomas, 40 malignant pleural mesotheliomas, 138 thymic tumours and 97 thyroid tumours) using the tissue microarray technique. Among thyroid tumours, the monoclonal and polyclonal PAX8 antibodies showed a high positive rate (98.0%). Of 167 polyclonal PAX8 antibody-positive tumours, except for thyroid tumours, 54 cases tested positive for PAX5 and/or PAX6 (31 lung carcinomas and 23 thymic tumours). No *PAX8* mRNA expression was detected using RNAscope (*in-situ* hybridization technique) other than in thyroid tumours. A portion of polyclonal PAX8 antibody-positive tumours showed cross-reactivity for PAX5 or PAX6 protein.

Conclusions: Monoclonal PAX8 antibody showed high specificity to thyroid tumours and was superior to the polyclonal antibody.

Keywords: cross-reactivity, immunohistochemistry, PAX8, thoracic tumours

Introduction

The lung is the most common site of metastasis for malignant tumours. The distinction of primary lung tumour from metastatic tumour is important, because the treatment modalities and prognosis for these two lesions are quite different. When lung tumours present with typical morphology the diagnosis is straightforward, and immunohistochemical staining is not necessary. However, poorly differentiated tumours are sometimes more challenging. Immunostaining for thyroid transcription factor-1 (TTF-1) is a useful positive marker for confirming adenocarcinoma of a unknown primary site as having a pulmonary origin. However, staining for TTF-1, as the name implies, is also positive in thyroid tumours.

The paired box transcription factor PAX8 is a nephric-lineage transcription factor. In human tissues, it is expressed in various normal tissues, such

Address for correspondence: K Tsuta, Division of Pathology and clinical Laboratories, National Cancer Center Hospital, 1-1 Tsukiji 5-chome, Chuo-ku, Tokyo 104-0045, Japan. e-mail: ktsuta@ncc.go.jp

as the thyroid gland, kidney and müllerian system, as well as in tumours arising in these regions. The usefulness of PAX8 in distinguishing ovarian serous tumours from malignant mesothelioma or renal collecting duct carcinoma from urothelial carcinoma has been reported.[1,2] In addition, PAX8 expression was reported in thymic neuroendocrine carcinomas,[3] normal B lymphocytes[4,5] and B cell lymphomas.[4]

However, some recent studies, mostly employing PAX8 polyclonal antibodies, have shown cross-reactivity with the B cell-specific transcription factor PAX5.[6,7] As a result, some previously reported PAX8 immunopositive normal tissues and tumours represented by B lymphocytes that did not express PAX8 mRNA could be considered to be due to this cross-reactivity, which has been attributed to the high sequence homology between PAX5 and PAX8 in the N-terminal region.[6] PAX8 polyclonal antibody was raised against a 212-amino acid-long polypeptide encompassing the N-terminal region of PAX8. In addition, a recent study revealed that one of the causes of aberrant polyclonal PAX8 positivity could be cross-reactivity for PAX6, which is crucial for neuronal development.[8]

The purpose of the present study was to compare the immunohistochemical staining profiles of PAX8-polyclonal, PAX8-monoclonal, PAX5-monoclonal and PAX6-monoclonal antibodies in several histological types of primary thoracic and thyroid tumours. In addition, we analysed *PAX8* mRNA expression by using *in-situ* hybridization with the novel, highly sensitive method of RNAscope.

Materials and Methods

CASE SELECTION AND CONSTRUCTION OF TISSUE MICROARRAYS

The institutional review board approved the study (2010-0077). The materials for the present study were extracted from cases deposited in the pathology files of the National Cancer Center Hospital, Tokyo. A total of 962 cases were used for the analysis; 687 lung carcinomas (253 adenocarcinomas; 158 squamous cell carcinomas; 106 large-cell neuroendocrine carcinomas; 67 small-cell carcinomas; 51 carcinoid tumours; 41 pleomorphic carcinomas; 11 large-cell carcinomas), 40 malignant pleural mesotheliomas (28 epithelioid; 12 biphasic), 138 thymic tumours (102 thymomas; 36 thymic carcinomas) and 97 thyroid tumours (80 papillary carcinomas; seven follicular carcinomas; five undifferentiated carcinomas; five follicular adenomas).

All diagnoses were based on conventional histopathological features evident in sections stained with haematoxylin and eosin, and using some specific stains, immunohistochemical and molecular techniques available at the time. Tissue microarray (TMA) utilized a core sample measuring 2.0 mm in diameter.

IMMUNOHISTOCHEMISTRY

For immunohistochemical staining, 4-μm-thick sections were deparaffinized and treated with 3% hydrogen peroxide for 30 min to block endogenous peroxidase activity, followed by washing in deionized water for 2–3 min. Heat-induced epitope retrieval with target retrieval solution high pH (Dako, Carpinteria, CA, USA) was performed. After the slides were allowed to cool at room temperature for 40 min, they were rinsed with deionized water and washed in phosphate-buffered saline for 5 min. The slides were then incubated with PAX8 polyclonal antibody (1:200; Proteintech, Chicago, IL, USA), PAX8 monoclonal antibody (PAX8R1, 1:50; Abcam, Cambridge, MA, USA), PAX5 monoclonal antibody (clone 24, 1:200; BD Biosciences, Franklin Lakes, NJ, USA) and PAX6 monoclonal antibody (P3U1, 1:500; Developmental Studies Hybridoma Bank, Iowa City, IA, USA) for 1 h at room temperature. Immunoreactions were detected using the Envision-plus system (Dako) and visualized with 3,3′-diaminobenzidine, followed by counterstaining with haematoxylin.

Immunohistochemical staining was scored independently by two observers (A.T. and K.T.). Nuclear staining was evaluated and the extent of staining (estimated percentage of stained cells) was recorded. Tumours were considered positive if >5% of the tumour nuclei were stained.

IN-SITU HYBRIDIZATION FOR *PAX8* MRNA

For detection of *PAX8* mRNA among polyclonal PAX8-antibody positive cases, an RNAscope FFPE Assay Kit (Advanced Cell Diagnostics, Inc., Hayward, CA, USA) and an RNAscope Probe Hs-PAX8 (Advanced Cell Diagnostics, Inc.) were used according to the manufacturer's instructions. Briefly, sections were pretreated with heat and protease. They were then incubated with the probe targeting *PAX8* for 2 h at 40°C. The slides were washed thoroughly with wash buffer (Advanced Cell Diagnostics, Inc.) after each hybridization step at room temperature. Diaminobenzidine was used as the chromogen. Sections were counterstained with haematoxylin. A probe for

POLR2A was used as a positive control. Positive staining was identified as brown, punctate spotting in the nucleus and/or cytoplasm.

Expression was scored using the instructions in the RNAscope FFPE Assay Kit: no staining (score 0); one to three dots/cell (score 1); four to 10 dots/cell (score 2); >10 dots/cell with 10% or less of positive cells having dot clusters (score 3); and >10 dots/cell with more than 10% of positive cells having dot clusters (score 4).

Results

REACTIVITY OF MONOCLONAL AND POLYCLONAL PAX8 ANTIBODIES

Immunoreactivity with the polyclonal PAX8 antibody was observed in 95 of 97 (98.0%) thyroid tumours [79 of 80 (98.8%) papillary carcinomas, seven (100%) follicular carcinomas, four of five (80.0%) undifferentiated carcinomas and five (100%) follicular adenomas]; as well as 55 of 687 (8.0%) lung carcinomas [six of 253 (2.4%) adenocarcinomas, three of 158 (1.9%) squamous cell carcinomas, 17 of 106 (16.0%) large-cell neuroendocrine carcinomas, 27 of 67 (40.3%) small-cell carcinomas, two of 11 (18.1%) large-cell carcinomas]; 91 of 102 (89.2%) thymomas; and 21 of 36 (58.3%) thymic carcinomas (Table 1). No malignant pleural mesotheliomas were positive using the polyclonal PAX8 antibody. Immunoreactivity with the monoclonal PAX8 antibody was observed in 95 of 97 (98.0%) cases of thyroid tumour: 78 of 80 (97.5%) papillary carcinomas, seven (100%) follicular carcinomas, five (100%) undifferentiated carcinomas, and five (100%) follicular adenoma; her tumours showed no reactivity.

When thyroid tumours were regarded as the gold standard for calculating the sensitivity of the PAX8 antibodies, the same sensitivity (98.0%) was observed for both monoclonal and polyclonal PAX8 antibodies.

Table 1. Positive cases stained with polyclonal PAX8, monoclonal PAX8, PAX5, and PAX6 antibodies

	Staining pattern in neoplastic cells, no. (%)			
Tumour types	PAX8 polyclonal	PAX8 monoclonal	PAX5	PAX6
Lung tumours				
Adenocarcinoma (n = 253)	6 (2.4)	0 (0)	0 (0)	26 (10.3)
Squamous cell carcinoma (n = 158)	3 (1.9)	0 (0)	0 (0)	29 (18.4)
Large cell neuroendocrine carcinoma (n = 106)	17 (16.0)	0 (0)	7 (6.6)	20 (18.9)
Small cell carcinoma (n = 67)	27 (40.3)	0 (0)	16 (23.9)	20 (29.9)
Carcinoid tumour (n = 51)	0 (0)	0 (0)	1 (2.0)	7 (13.7)
Pleomorphic carcinoma (n = 41)	0 (0)	0 (0)	0 (0)	2 (4.9)
Large cell carcinoma (n = 11)	2 (18.1)	0 (0)	0 (0)	3 (27.3)
Malignant pleural mesothelioma (n = 40)	0 (0)	0 (0)	0 (0)	5 (12.5)
Thymic tumours				
Thymoma (n = 102)	91 (89.2)	0 (0)	0 (0)	16 (15.7)
Thymic carcinoma (n = 36)	21 (58.3)	0 (0)	7 (19.4)	4 (11.1)
Thyroid tumours				
Papillary carcinoma (n = 80)	79 (98.8)	78 (97.5)	0 (0)	0 (0)
Follicular carcinoma (n = 7)	7 (100)	7 (100)	0 (0)	1 (14.3)
Undifferentiated carcinoma (n = 5)	4 (80.0)	5 (100)	0 (0)	2 (40.0)
Follicular adenoma (n = 5)	5 (100)	5 (100)	0 (0)	0 (0)

However, compared to the polyclonal antibody, the monoclonal antibody showed lower intensity and percentage of positive cells (Figure 1A,B).

REACTIVITY OF PAX5 AND PAX6 ANTIBODIES

PAX5 immunoreactivity was observed in 24 (3.5%) cases of lung carcinoma [seven (6.6%) large-cell neuroendocrine carcinomas, 16 (23.9%) small-cell carcinomas, and one (2.0%) carcinoid tumour]; and seven (19.4%) thymic carcinomas (Figure 2). Thyroid tumours, lung carcinomas except for neuroendocrine tumours, malignant pleural mesotheliomas and thymomas were negative for PAX5.

PAX6 staining was positive in three (3.1%) cases of thyroid tumour [one (14.3%) follicular carcinoma and two (40.0%) undifferentiated carcinomas]; 107 (15.6%) cases of lung carcinoma [26 (10.3%) adenocarcinomas, 29 (18.4%) squamous cell carcinomas, two (4.9%) pleomorphic carcinomas, 20 (18.9%) large-cell neuroendocrine carcinomas, 20 (29.9%) small-cell carcinomas, three (27.3%) large-cell carcinomas, and seven (13.7%) carcinoid tumours]; five (12.5%) malignant pleural mesotheliomas; and 20 (14.5%) thymic tumours.

CROSS-REACTIVITY AMONG POLYCLONAL PAX8, PAX5 AND PAX6 ANTIBODIES

Among the 95 polyclonal PAX8 antibody-positive thyroid tumours, PAX5 and/or PAX6 staining was positive in only two (2.1%) cases. In contrast, among the 167 polyclonal PAX8 antibody-positive tumours other than thyroid tumours, PAX5 and/or PAX6

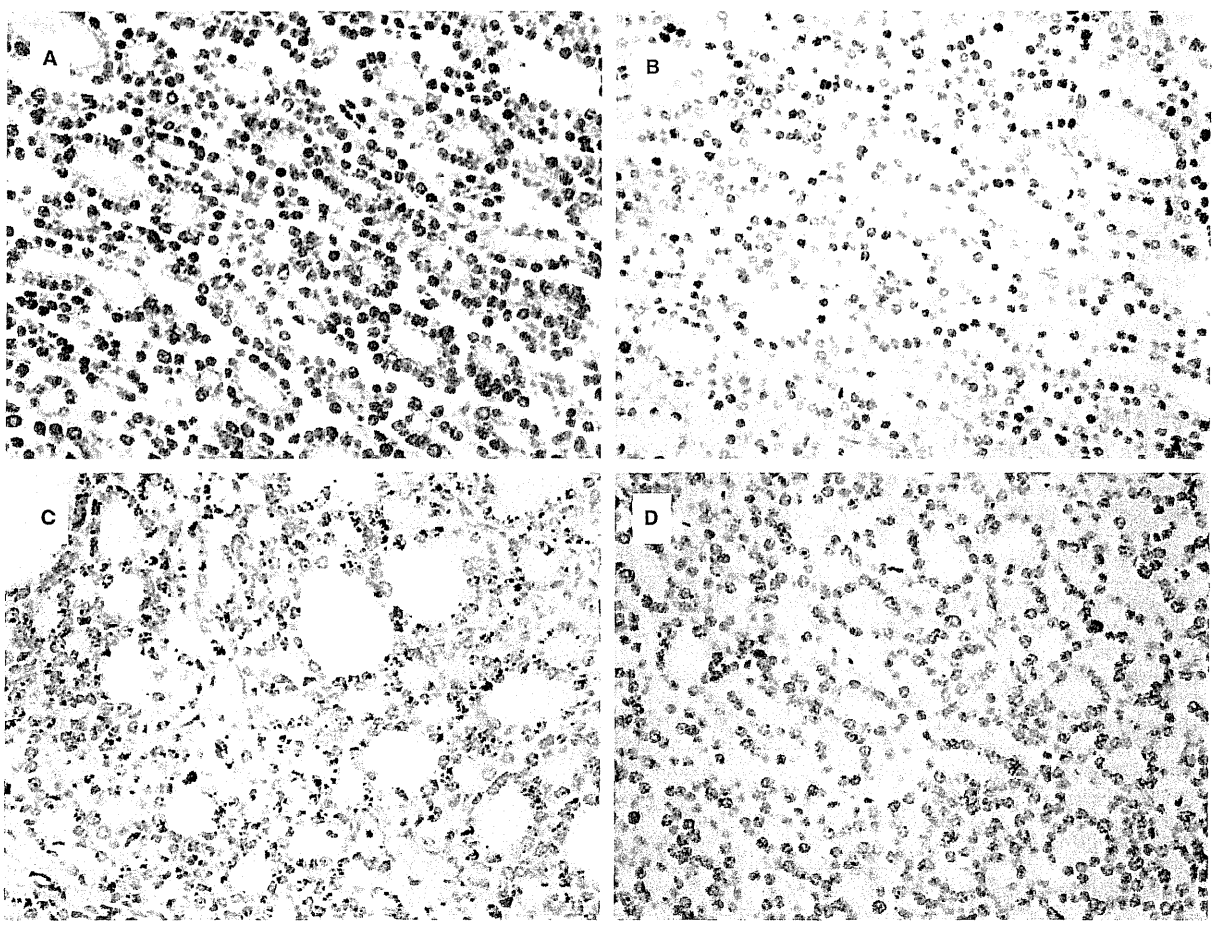

Figure 1. Follicular carcinoma immunoreactivity. **A**, Diffuse, strong positive staining using polyclonal PAX8 antibody. **B**, Staining with the monoclonal PAX8 antibody shows more focal and weaker staining than with the polyclonal antibody. **C**, *PAX8* mRNA *in-situ* hybridization shows dot-like staining and clusters. **D**, *POLR2A* mRNA *in-situ* hybridization shows dot-like staining.

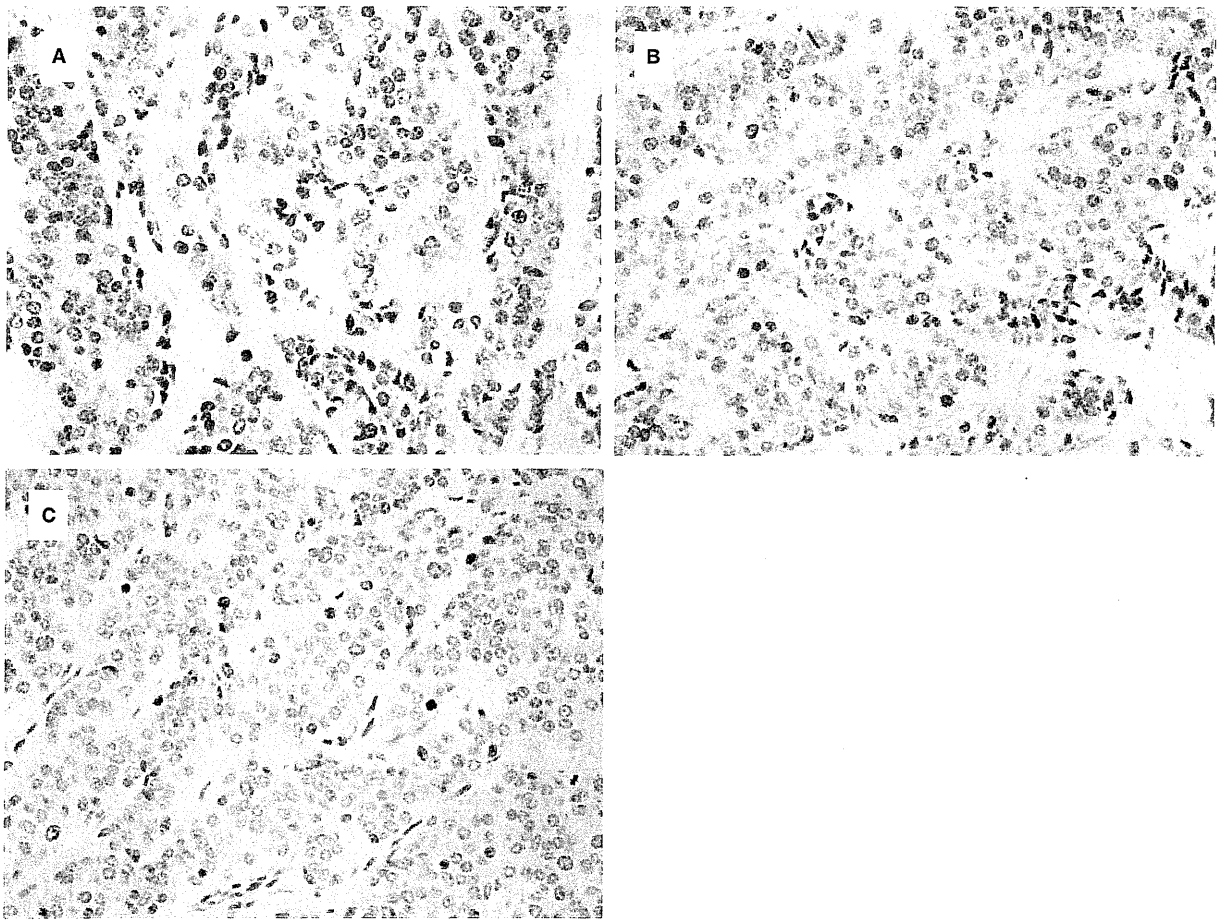

Figure 2. Thymic carcinoma immunoreactivity. **A**, Diffuse, moderate staining with the polyclonal PAX8 antibody. **B**, PAX 5 antibody shows similar, but weaker, positive staining patterns than PAX8. **C**, Tumour cells are focally positive for PAX6.

staining was positive in 54 (32.3%) cases. In detail, PAX 5 staining was positive in 16 lung carcinomas (four of 17 large-cell neuroendocrine carcinomas and 12 of 27 small-cell carcinomas) and seven of 21 thymic carcinomas (Figure 2A–C). PAX6 staining was positive in 20 lung carcinomas (one of six adenocarcinomas, three of three squamous cell carcinomas, eight of 17 large-cell neuroendocrine carcinomas, eight of 27 small-cell carcinomas) and 18 of 112 thymic tumours (16 of 91 thymomas and two of 21 thymic carcinomas). The overlapping cases are depicted as Venn diagrams (Figure 3).

PAX8 MRNA EXPRESSION

To confirm that aberrant PAX8 detection was induced by cross-reactivity of other protein expression, we evaluated *PAX8* mRNA expression using an *in-situ* hybridization technique. Among 262 polyclonal PAX8 antibody-positive cases, 18 were negative for *POLR2A* mRNA, which was considered to indicate insufficient material for mRNA evaluation; thus, the final cohort for *in-situ* hybridization for *PAX8* mRNA analysis consisted of 244 cases (93.1%); that is, 89 thyroid tumours and 155 non-thyroid tumours. Among the 244 analysed cases, 85 (34.8%) were positive for *PAX8* mRNA expression. All *PAX8* mRNA-positive cases were the thyroid tumours, and they constituted 95.5% of the *POLR2A* mRNA positive thyroid tumours (Figure 1C,D).

Discussion

The current study showed that the monoclonal PAX8 antibody was a highly specific marker and equally

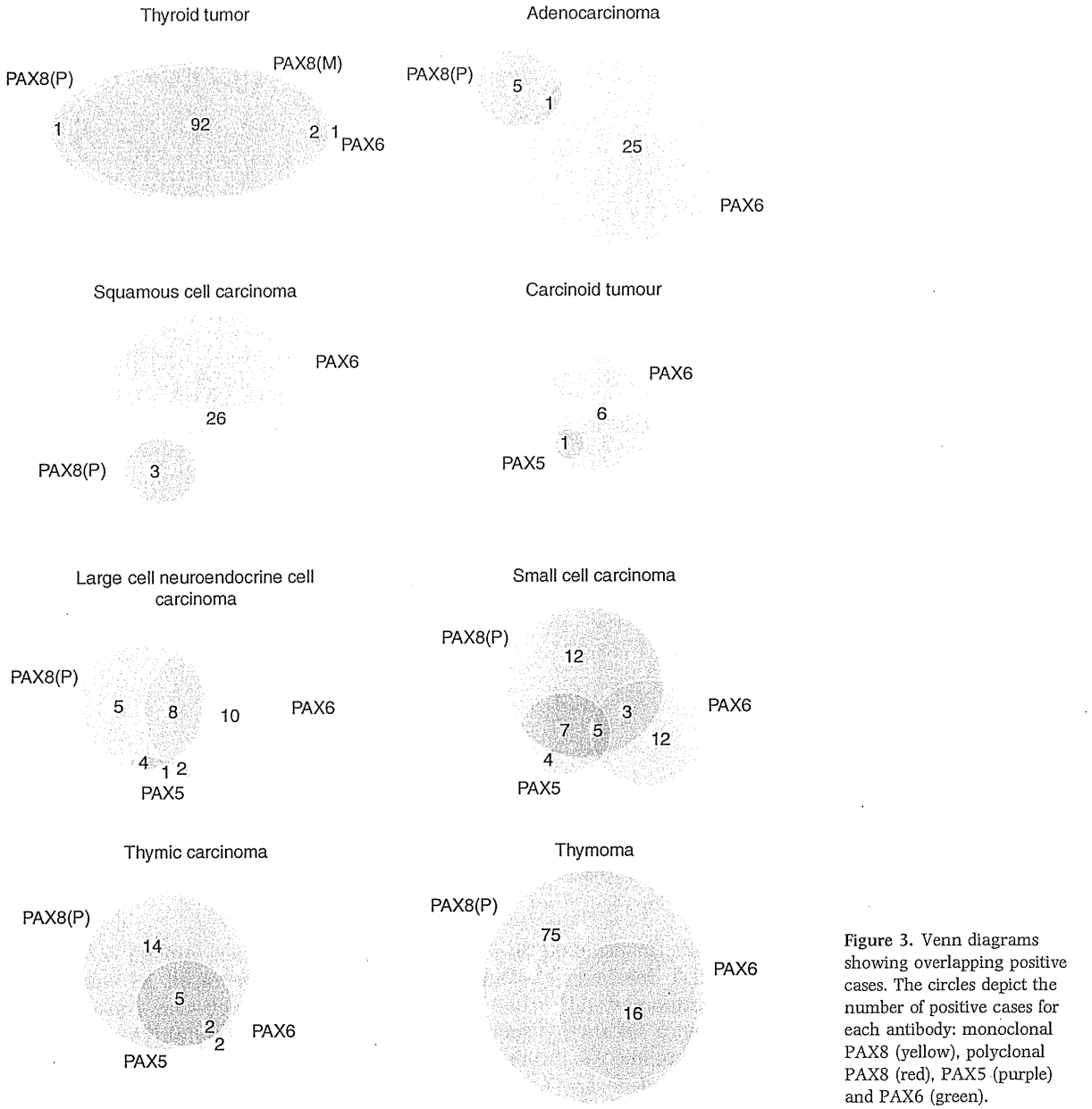

Figure 3. Venn diagrams showing overlapping positive cases. The circles depict the number of positive cases for each antibody: monoclonal PAX8 (yellow), polyclonal PAX8 (red), PAX5 (purple) and PAX6 (green).

sensitive compared to polyclonal PAX8 antibody. In addition, the aberrant detection by polyclonal PAX8 was partially caused by cross-reactivity with PAX5 and/or PAX6.

When thyroid tumours were regarded as the gold standard for calculating the sensitivity for PAX8, the monoclonal PAX8 antibody showed a high positive detection rate, identical to that of the polyclonal antibody. When compared with the findings of the present study, identical sensitivity was observed for polyclonal and monoclonal PAX8 antibodies in ovarian serous carcinoma.[9] Conversely, monoclonal PAX8 antibody showed higher sensitivity in ovarian endometrioid and renal cell carcinomas, which were regarded as the gold standard in the same study.[9] These conflicting results for the detection of PAX8 expression may be due to differences in target organ, scoring system or possibly staining techniques with different antigen-retrieval methods. In general, the immunoreactivity of the monoclonal antibody was

lower compared with that of the polyclonal one because the monoclonal antibody recognizes a single epitope, whereas the polyclonal antibody can recognize multiple epitopes and is less likely to be affected by changes in protein conformation.[10]

Similar to previous reports,[3,11,12] 81.2% of cases of thymic tumour and 25.4% of cases of pulmonary neuroendocrine carcinoma showed polyclonal PAX8 reactivity, and PAX8 was not detected in cases of pulmonary carcinoid tumour. However, these observations were attributed to the cross-reactivity of the polyclonal PAX8 antibody because detection using monoclonal PAX8 was negative in these tumours. Previous studies suggested a similar reactivity pattern (positive with polyclonal PAX8 but negative with monoclonal PAX8) and these reactions observed in B cell lymphomas were considered to be caused by antibody cross-reactivity.[6,7,9]

As described above, the cross-reactivity with PAX5 or PAX6 protein was one of the known reasons for aberrant staining with polyclonal PAX8 antibody.[6–8] However, a proportion of polyclonal PAX8 antibody-positive lung and thymic tumours showed PAX5 protein expression. In addition, PAX6 expression was limited in a proportion of polyclonal PAX8 antibody-positive lung and thymic tumours. The possibility of cross-reactivity with other PAX families of similar structures needs to be considered, because *PAX* gene family members share similar sequence homology.[13] In fact, cross-reactivity between PAX2 protein and PAX5 antibody has been reported.[14]

We observed that *PAX8* mRNA expression was not observed among polyclonal PAX8-positive tumours other than those in the thyroid. Although mRNA expression is not always parallel to protein expression, the current data reinforce the hypothesis that polyclonal PAX8-positive tumours, other than those in the thyroid, are not showing genuine PAX8 protein expression.[6] To reduce the possibility of false-negative results with the currently used immunohistochemical technique, we used commercially available kits and probes. In addition, the currently used method is highly sensitive for the detection of a small mRNA copy number from the formalin-fixed, paraffin-embedded samples. Finally, we excluded cases that tested negative for the expression of *POLR2A* mRNA internal control. This result indicated that the difference in the positive results for polyclonal and monoclonal PAX8 antibodies in tumours, other than those in the thyroid, was not induced by reduced sensitivity of PAX8 monoclonal antibody.

The utility of PAX5 and PAX6 antibodies for solid organs is limited, because PAX5 expression was positive in a proportion of pulmonary neuroendocrine tumours and thymic carcinomas. However, PAX5 expression may be useful in distinguishing pulmonary neuroendocrine tumours from poorly differentiated non-neuroendocrine carcinomas. In agreement with previous reports, pulmonary small-cell carcinoma showed high PAX5 antibody reactivity compared with other low-grade pulmonary neuroendocrine tumours.[15–17] Although PAX6 expression was reported in pancreatic neuroendocrine tumours[8] and the neuroepidermis,[18] the present data indicate that such expression is not high and is restricted to pulmonary neuroendocrine tumours.

In conclusion, the monoclonal PAX8 antibody is highly specific as a thyroidal cell marker, and equally as sensitive as the polyclonal PAX8 antibody; it would be better suited, in daily practice, for identification of PAX8-expressing tumours.

Acknowledgements

We would like to thank Sachiko Miura MT, Chizu Kina MT and Mr Ryousuke Yamaga for their skillful technical assistance. This work was supported in part by the National Cancer Center Research and Development Fund (23-A-2), (23-A-11), (23-A-35) and (24-A-1) and by a Grant-in-Aid for Scientific Research (C) (grant number 25460446).

Conflict of interest

The authors declare that they have no potential or actual conflicts of interest.

References

1. Laury AR, Hornick JL, Perets R *et al.* PAX8 reliably distinguishes ovarian serous tumours from malignant mesothelioma. *Am. J. Surg. Pathol.* 2010; 34; 627–635.
2. Albadine R, Schultz L, Illei P *et al.* PAX8 (+)/p63 (−) immunostaining pattern in renal collecting duct carcinoma (CDC): a useful immunoprofile in the differential diagnosis of CDC versus urothelial carcinoma of upper urinary tract. *Am. J. Surg. Pathol.* 2010; 34; 965–969.
3. Haynes CM, Sangoi AR, Pai RK. PAX8 is expressed in pancreatic well-differentiated neuroendocrine tumours and in extrapancreatic poorly differentiated neuroendocrine carcinomas in fine-needle aspiration biopsy specimens. *Cancer Cytopathol.* 2011; 119; 193–201.
4. Ozcan A, Shen SS, Hamilton C *et al.* PAX8 expression in non-neoplastic tissues, primary tumours, and metastatic tumours: a

comprehensive immunohistochemical study. *Mod. Pathol.* 2011; 24; 751–764.
5. Laury AR, Perets R, Piao H *et al.* A comprehensive analysis of PAX8 expression in human epithelial tumours. *Am. J. Surg. Pathol.* 2011; 35; 816–826.
6. Moretti L, Medeiros LJ, Kunkalla K, Williams MD, Singh RR, Vega F. N-terminal PAX8 polyclonal antibody shows cross-reactivity with n-terminal region of PAX5 and is responsible for reports of PAX8 positivity in malignant lymphomas. *Mod. Pathol.* 2012; 25; 231–236.
7. Morgan EA, Pozdnyakova O, Nascimento AF, Hirsch MS. PAX8 and PAX5 are differentially expressed in B-cell and T-cell lymphomas. *Histopathology* 2013; 62; 406–413.
8. Lorenzo PI, Jimenez Moreno CM, Delgado I *et al.* Immunohistochemical assessment of PAX8 expression during pancreatic islet development and in human neuroendocrine tumours. *Histochem. Cell Biol.* 2011; 136; 595–607.
9. Tacha D, Qi W, Zhou D, Bremer R, Cheng L. PAX8 mouse monoclonal antibody [bc12] recognizes a restricted epitope and is highly sensitive in renal cell and ovarian cancers but does not cross-react with B cells and tumours of pancreatic origin. *Appl. Immunohistochem. Mol. Morphol.* 2013; 21; 59–63.
10. Lane D, Koprowski H. Molecular recognition and the future of monoclonal antibodies. *Nature* 1982; 296; 200–202.
11. Weissferdt A, Moran CA. PAX8 expression in thymic epithelial neoplasms: an immunohistochemical analysis. *Am. J. Surg. Pathol.* 2011; 35; 1305–1310.
12. Sangoi AR, Ohgami RS, Pai RK, Beck AH, McKenney JK, Pai RK. PAX8 expression reliably distinguishes pancreatic well-differentiated neuroendocrine tumours from ileal and pulmonary well-differentiated neuroendocrine tumours and pancreatic acinar cell carcinoma. *Mod. Pathol.* 2011; 24; 412–424.
13. Robson EJ, He SJ, Eccles MR. A panorama of PAX genes in cancer and development. *Nat. Rev. Cancer* 2006; 6; 52–62.
14. Morgenstern DA, Hasan F, Gibson S, Winyard P, Sebire NJ, Anderson J. PAX5 expression in nonhematopoietic tissues. Reappraisal of previous studies. *Am. J. Clin. Pathol.* 2010; 133; 407–415.
15. Song J, Li M, Tretiakova M, Salgia R, Cagle PT, Husain AN. Expression patterns of PAX5, c-met, and paxillin in neuroendocrine tumours of the lung. *Arch. Pathol. Lab. Med.* 2010; 134; 1702–1705.
16. Sica G, Vazquez MF, Altorki N *et al.* PAX-5 expression in pulmonary neuroendocrine neoplasms: its usefulness in surgical and fine-needle aspiration biopsy specimens. *Am. J. Clin. Pathol.* 2008; 129; 556–562.
17. Kanteti R, Nallasura V, Loganathan S *et al.* PAX5 is expressed in small-cell lung cancer and positively regulates c-met transcription. *Lab. Invest.* 2009; 89; 301–314.
18. Abiko K, Mandai M, Hamanishi J *et al.* Oct4 expression in immature teratoma of the ovary: relevance to histologic grade and degree of differentiation. *Am. J. Surg. Pathol.* 2010; 34; 1842–1848.

Cancer Medicine

ORIGINAL RESEARCH

Copy number increase of *ACTN4* is a prognostic indicator in salivary gland carcinoma

Yukio Watabe[1,2], Taisuke Mori[3], Seiichi Yoshimoto[4], Takeshi Nomura[2], Takahiko Shibahara[2], Tesshi Yamada[1] & Kazufumi Honda[1]

[1]Division of Chemotherapy and Clinical Research, National Cancer Center Research Institute, Tokyo 104-0045, Japan
[2]Department of Oral and Maxillofacial Surgery, Tokyo Dental College, Chiba 261-8502, Japan
[3]Division of Molecular Pathology, National Cancer Center Research Institute, Tokyo 104-0045, Japan
[4]Department of Head and Neck Oncology, National Cancer Center Hospital, Tokyo 104-0045, Japan

Keywords
Actinin-4, *ACTN4*, head and neck cancer, prognostic marker, salivary gland carcinoma

Correspondence
Kazufumi Honda, Division of Chemotherapy and Clinical Research, National Cancer Center Research Institute, 5-1-1 Tsukiji, Chuo-ku, Tokyo 104-0045, Japan.
Tel: +81-3-3542-2511; Fax: +81-3-3547-6045;
E-mail: khonda@ncc.go.jp

Funding Information
This work was supported by a Grant-in Aid for Scientific Research (B) and a Challenging Exploratory Research from the Ministry of Education, Culture, Sports, Science and Technology (METX) of Japan (K. H.), and the National Cancer Center Research and Development Fund (23-A-38, and 23-A-11) (K. H.).

Received: 10 December 2013; Revised: 23 January 2014; Accepted: 28 January 2014

doi: 10.1002/cam4.214

Abstract

Copy number increase (CNI) of *ACTN4* has been associated with poor prognosis and metastatic phenotypes in various human carcinomas. To identify a novel prognostic factor for salivary gland carcinoma, we investigated the copy number of *ACTN4*. We evaluated DNA copy number of *ACTN4* in 58 patients with salivary gland carcinoma by using fluorescent in situ hybridization (FISH). CNI of *ACTN4* was recognized in 14 of 58 patients (24.1%) with salivary gland carcinoma. The cases with CNI of *ACTN4* were closely associated with histological grade ($P = 0.047$) and vascular invasion ($P = 0.033$). The patients with CNI of *ACTN4* had a significantly worse prognosis than the patients with normal copy number of *ACTN4* ($P = 0.0005$ log-rank test). Univariate analysis by the Cox proportional hazards model showed that histological grade, vascular invasion, and CNI of *ACTN4* were independent risk factors for cancer death. Vascular invasion (hazard ratio [HR]: 7.46; 95% confidence interval [CI]: 1.98–28.06) and CNI of *ACTN4* (HR: 3.23; 95% CI: 1.08–9.68) remained as risk factors for cancer death in multivariate analysis. Thus, CNI of *ACTN4* is a novel indicator for an unfavorable outcome in patients with salivary gland carcinoma.

Introduction

Salivary gland carcinomas are rare malignant tumors comprising about 5% of cancers of the head and neck region [1]. In addition, the histopathology of salivary gland tumors is diverse. The classification system of the World Health Organization (WHO) contains at least 24 histopathological types of salivary gland carcinomas. The management of salivary gland carcinomas can be confusing due to the extreme diversity of tumor types, their relative rarity, the requirement for long-term follow-up, and strategy for treatment in many instances to predict outcome. Although the clinical parameters, such as clinical stage, age, and tumor location, are important for the

prognostic factors in salivary gland carcinoma, histological grading also ranks highly as a critical prognostic factor. Histological grading may stratify the risk of lymph node metastasis and give a rationale for the extent of surgery and the need for adjuvant therapy [2]. If surrogate biomarkers associated with histological grade and/or outcome could be identified, they would become powerful indicators of the optimal treatment strategy for patients with salivary gland carcinoma.

We identified actinin-4, an actin-bundling protein encoded by *ACTN4*, as a biomarker that could be used to evaluate the invasion and metastasis capabilities of cancer cells [3]. The overexpression of actinin-4 proteins was closely associated with the invasive phenotypes of some cancers, such as breast [3], colorectal [4, 5], ovarian [6, 7], bladder [8, 9], oral squamous cell [10], pancreas [11, 12], and lung carcinomas [13–15]. Oncogene amplification is often observed in aggressive malignant phenotypes of cancer [16]. Recently, it has been reported that the amplification of *ACTN4* can strictly predict the clinical outcome, and *ACTN4* has been recognized as an oncogene [6, 11, 13].

In the present study, we investigated the copy number of *ACTN4* in salivary gland carcinomas by using fluorescent in situ hybridization (FISH). Copy number increase (CNI) of *ACTN4* was positively associated with histological grade and poor outcome. We identified the biomarker to predict the outcome of salivary gland carcinoma.

This is the first report to examine the clinical usage of CNI of *ACTN4* as a prognostic factor in salivary gland carcinoma.

Patients and Methods

Patients and tissue samples

We reviewed the clinicopathological records of 58 patients who underwent surgical resection with curative intention for salivary gland carcinoma at the National Cancer Center Central Hospital (Tokyo, Japan) between 1997 and 2011.

Formalin-fixed paraffin-embedded tissue samples of 58 salivary gland carcinomas and 10 normal submandibular gland or parotid gland specimens were collected and reviewed in our institution (T. M.) according to the WHO classification of salivary gland carcinomas (Table 1). Histological grade was determined according to the three-tiered grading system proposed by Jouzdani [17].

This study was approved by the ethics committee of the National Cancer Center (approval #2010-0759).

TMA construction

Tissue microarrays (TMAs) were prepared from formalin-fixed paraffin-embedded pathological blocks, as previously described [18]. TMA blocks were cut into 4-μm-thick sections and subjected to FISH and immunohistochemistry (IHC) [4, 11].

Fluorescence in situ hybridization

The FISH probe of bacterial artificial chromosome clone containing *ACTN4* and chromosome 19p (a control clone) was purchased from Abnova (Taipei, Taiwan) [13].The labeled bacterial artificial chromosome clone DNA was subjected to FISH as previously described. TMAs were hybridized with FISH probes at 37°C for 48 h. The nuclei were counterstained with 4, 6-duamidino-2-phenylindone. The number of fluorescence signals corresponding to the copy number of *ACTN4* and control signals in the nuclei of 20 interphase tumor cells was counted (Y. W. and K. H.).

FISH patterns were defined as described previously [19, 20]. Briefly, the samples were grouped as normal disomy (two or less *ACTN4* signals in more than 90% of cells), low polysomy (four or more *ACTN4* signals in more than 10% but less than 40% of tumor cells), high polysomy (four or more *ACTN4* signals in more than 40% of tumor cells), and gene amplification (ratio *ACTN4*/chromosome more than 2, or 15 copies in more than 10% of tumor cells) [19, 20].

Immunohistochemistry

The anti-actinin-4 monoclonal antibody (13G9), which we originally established, was purchased from Transgenic Inc. (Kumamoto, Japan) [14]. Immunostaining of actinin-4 proteins was performed with the Ventana DABMap detection kit and an automated slide stainer (Discovery XT; Ventana Medical System, Tucson, AZ) [13, 14]. The expression level of actinin-4 protein was classified as: no expression (immunoreactivity score, 0), in which no tumor cells were stained with anti-actinin-4 antibody; weak expression (+1), in which tumor cells were stained with weaker intensity than endothelial cells; moderate expression (+2), in which less than 30% of tumor cells were stained; and strong expression (+3), in which more than 30% of tumor cells were stained. Two independent investigators (Y. W. and T. M.) who had no clinical information about the cases evaluated the staining patterns.

Statistical analysis

Significant differences were detected by using the Mann–Whitney *U* test, Student's *t*-test, Pearson's chi-square test, and Fisher's exact test. Overall survival was measured as the period from surgery to the date of death or last follow-up and was estimated by the Kaplan–Meier analysis. Differences between the overall survival curves were

Table 1. Association of *ACTN4* with clinicopathological characteristics of salivary gland cancer patients.

	ACTN4 FISH			Actinin-4 IHC		
	NCN	CNI	*P*-value	Negative (0, +1)	Positive (+2, +3)	*P*-value
Total	44 (75.9%)	14 (24.1%)		19 (32.8%)	39 (67.2%)	
ADCC	20 (95.2%)	1 (4.8%)		3 (14.3%)	18 (85.7%)	
CAEPA	8 (72.7%)	3 (27.3%)		5 (45.5%)	6 (54.5%)	
EMYC	2 (66.7%)	1 (33.3%)		0	3 (100%)	
MYC	0	1 (100%)		1 (100%)	0	
ACCC	3 (100%)	0		1 (33.3%)	2 (66.7%)	
ACNOS	5 (71.4%)	2 (28.6%)		4 (57.1%)	3 (42.9%)	
MEC	3 (75.0%)	1 (25.0%)		2 (50.0%)	2 (50.0%)	
SDC	2 (50.0%)	2 (50.0%)		2 (50.0%)	2 (50.0%)	
SC	1 (33.3%)	2 (66.7%)		0	3 (100%)	
OC	0	1 (100%)		1 (100%)	0	
Age						
<67 years	26 (83.9%)	5 (16.1%)	0.1267	9 (29.0%)	22 (71.0%)	0.5170
≥67 years	18 (66.7%)	9 (33.3%)		10 (37.0%)	17 (63.0%)	
Gender						
Men	24 (75.0%)	8 (25.0%)	0.8648	13 (40.6%)	19 (59.4%)	0.1567
Women	20 (76.9%)	6 (23.1%)		6 (23.1%)	20 (76.9%)	
Size						
T1–T2	12 (100%)	0	0.0503	4 (33.3%)	8 (66.7%)	1.000
T3–T4	28 (68.3%)	13 (31.7%)		14 (34.1.%)	27 (65.9%)	
Unknown	4 (80.0%)	1 (20.0%)		1 (20.0%)	4 (80.0%)	
Lymph node metastasis						
Absent	31 (79.5%)	8 (20.5%)	0.5141	10 (25.6%)	29 (74.4%)	0.0980
Present	13 (68.4%)	6 (31.6%)		9 (47.4%)	10 (52.6%)	
Histological grade						
Low, intermediate	**26 (86.7%)**	**4 (13.3%)**	**0.0465***	7 (23.3%)	23 (76.7%)	0.1134
High	**18 (64.3%)**	**10 (35.7%)**		12 (42.9%)	16 (57.1%)	
Neural invasion						
Absent	23 (76.7%)	7 (23.3%)	0.8822	11 (36.7%)	19 (63.3%)	0.5116
Present	21 (75.0%)	7 (25.0%)		8 (28.6%)	20 (71.4%)	
Vascular invasion						
Absent	**36 (83.7%)**	**7 (16.3%)**	**0.0326***	13 (29.5%)	31 (70.5%)	0.5141
Present	**8 (53.3%)**	**7 (46.7%)**		6 (42.9%)	8 (57.1%)	

FISH, fluorescent in situ hybridization; IHC, immunohistochemistry; ADCC, adenoid cystic carcinoma; CAEPA, carcinoma ex pleomorphic adenoma; EMYC, epithelial-myoepithelial carcinoma; MYC, myoepithelial carcinoma; ACCC, acinic cell carcinoma; ACNOS, adenocarcinoma, not otherwise specified; MEC, mucoepidermoid carcinoma; SDC, salivary duct carcinoma; SC, sebaceous carcinoma; OC, oncocytic carcinoma; NCN, normal copy number; CNI, copy number increase.

*$P < 0.05$. Statistically significant associations are highlighted in bold.

assessed with the log-rank test. Univariate and multivariate analyses were performed with the Cox regression model. Data were analyzed with the StatFlex statistical software package (version 6.0; Artiteck, Osaka, Japan) or the R-project (http://www.r-project.org/) [11, 13, 14].

Results

Determination of the copy number of *ACTN4* by FISH

We determined the copy number of *ACTN4* in salivary gland carcinomas by using FISH. Among the 58 tumors, 33 exhibited normal disomy (56.9%), 11 exhibited low polysomy (19.0%), 10 exhibited high polysomy (17.2%), and four exhibited gene amplification (6.9%) (Table 1). Tumors with normal disomy and low polysomy were defined as having normal copy number (NCN) of *ACTN4*, and tumors with high polysomy and gene amplification were defined as having a CNI of *ACTN4*, according to the definition of FISH analysis for epidermal growth factor receptor 1 (*EGFR*) (Fig. 1A and B). Fourteen of 58 tumors (24.1%) exhibited CNI, and 44 of 58 tumors exhibited NCN (75.9%). Histologically, the CNI was recognized in adenoid cystic carcinoma (ADCC) (4.8%, 1/21), carcinoma ex pleomorphic adenoma

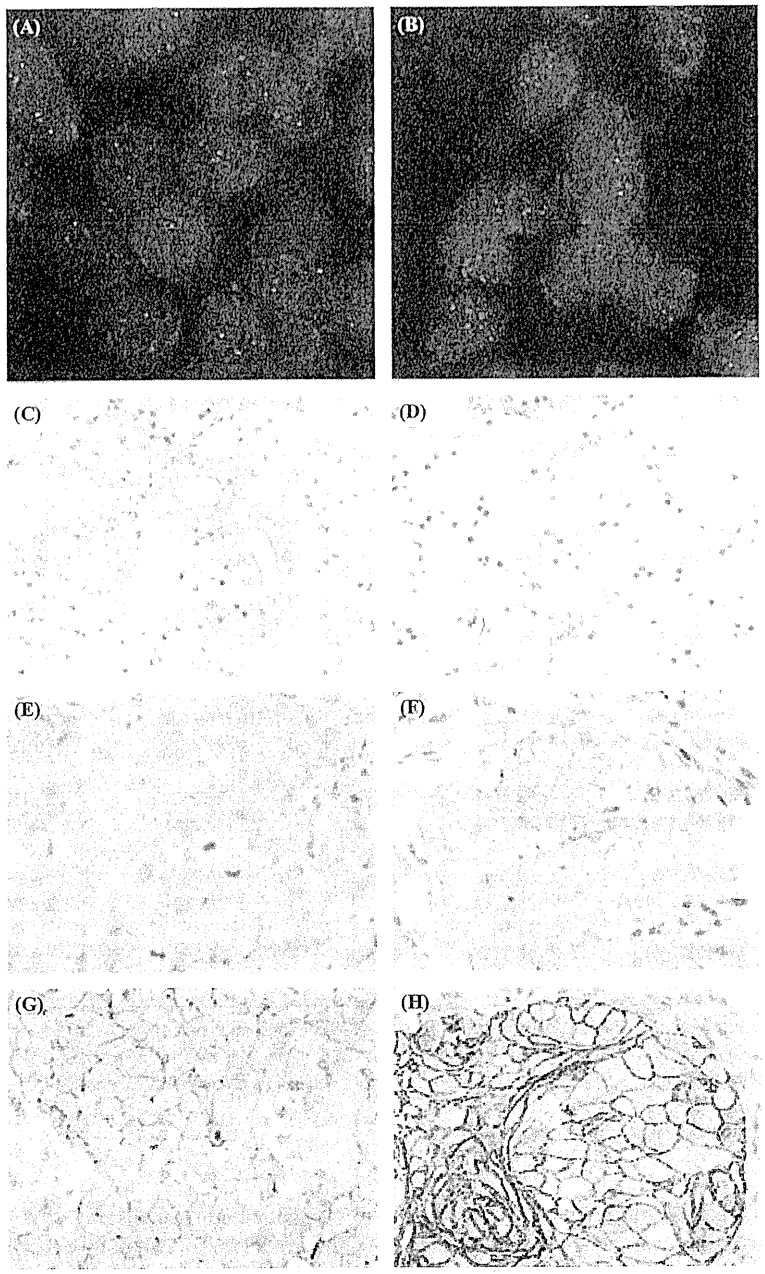

Figure 1. Representative copy number status of *ACTN4* in salivary gland cancer determined by fluorescence in situ hybridization (FISH) (A and B). Representative expression of actinin-4 protein in normal salivary gland (C and D) and salivary gland cancer (E–H), as determined by immunohistochemistry (IHC). (A) Disomy of *ACTN4* in an adenoid cystic carcinoma (ADCC), (B) gene amplification of *ACTN4* in ADCC. (C) striated duct, (D) acinar gland, (E) no expression of actinin-4 protein in mucoepidermoid carcinoma (immunoreactivities score 0), (F) weak expression, in salivary duct carcinoma (+1), (G) moderate expression in salivary duct carcinoma (+2), (H) strong expression in sebaceous carcinoma (+3).

(CAEPA) (3/11, 27.3%), epithelial-myoepithelial carcinoma (EMYC) (1/3, 33.3%), myoepithelial carcinoma (MYC) (1/1, 100%), adenocarcinoma not otherwise specified (ACNOS) (2/7, 28.6%), mucoepidermoid carcinoma (MEC) (1/4, 25.0%), salivary duct carcinoma (SDC) (2/4, 50%), sebaceous carcinoma (SC) (2/3, 66.7%) and oncocytic carcinoma (OC) (1/1 100%). The NCN and CNI groups had statistically significant differences in